ALA-Porphyrin Science

Enhancing Effect of Novel Schiff Base Derivatives, UTX-134 and UTX-135, on 5-Aminolevulinic Acid-based Photodynamic Therapy

Hirari Yamahana[a], Yusei Shinohara[a], Yoshio Endo[b], Tohru Obata[c], Hisatsugu Yamada[a] and Yoshihiro Uto[a]*

[a] *Graduate School of Technology, Industrial and Social Science, Tokushima University, Tokushima, Japan*
[b] *Central Research Resource Branch, Cancer Research Institute, Kanazawa University, Kanazawa, Japan*
[c] *School of Pharmaceutical Sciences, Aichi Gakuin University, Nagoya, Japan.*
[*] *Corresponding Author, Fax/Tel: +81-88-656-7514; E-mail: uto.yoshihiro@tokushima-u.ac.jp*

Received in 16th August 2021, Accepted 31st August 2021

Summary

5-Aminolevulinic acid (ALA) is a precursor of protoporphyrin IX (PpIX), which is a potent intracellular photosensitizer for photodynamic therapy (PDT). PpIX is biosynthesized from ALA by enzymatic modifications through the heme synthesis pathway. We have previously shown that TX-816 clearly increased the effect of PDT using ALA (ALA-PDT). We found that TX-816 derivatives in which 2-chloro-4-nitroaniline (CNA) was substituted with 4-pentyl or 4-hexyl aniline (UTX-127 and UTX-128) were more stable than TX-816 in an aqueous solution. We examined the ALA-PDT-enhancing effects of the novel 4-alkyl aniline derivatives, which were synthesized from 4-methoxysalicylaldehyde (MeOSA), and 4-alkyl anilines with various alkyl chains from C=0 to C=6 (UTX-128 to UTX-135). MeOSA-based 4-alkyl aniline derivatives or 3,5-dichlorosalicylaldehyde (DCSA)-based 4-alkyl aniline derivatives, specifically MeOSA-based 4-pentyl and 4-hexyl aniline derivatives (UTX-134 and UTX-135), showed a strong ALA-PDT-enhancing effect. These results indicated that MeOSA-based 4-pentyl and 4-hexyl aniline derivatives are potent lead compounds for the development of an ALA-PDT sensitizer.

Keywords:
5-Aminolevulinic acid (ALA), Protoporphyrin IX (PpIX), Photodynamic therapy (PDT), Schiff base

Introduction

Photodynamic therapy (PDT) is a therapeutic method in which cells are denatured and necrotized by irradiating the tissue with laser after the administration of a photosensitizer [1]. The denaturation and necrosis are due to the strong oxidative effect of reactive oxygen species generated by the reaction between the laser light and the photosensitive agent.

5-Aminolevulinic acid (ALA) is biosynthesized by 5-aminolevulinate synthetase from succinyl-CoA and glycine [2]. As ALA is an intermediate precursor in the heme biosynthesis pathway, the exogenous administration of ALA in patients leads to the selective accumulation of protoporphyrin IX (PpIX) within malignant tissues [3,4]. Intracellular PpIX accumulated in cancer cells emits red fluorescence (635 nm) upon excitation with blue light (λ = 400–410 nm). In contrast,

PpIX exposed to red light (λ = 630–700 nm) produces reactive oxygen species that results in cell death of various cancer cells [5–7].

The former characteristic of ALA can be used to diagnose tumors (intraoperative photodynamic diagnosis, ALA-PDD), and its latter property can be applied to the treatment of various diseases as a less invasive therapy (ALA-PDT). ALA-PDD is now widely used for malignant glioma and bladder cancer [8,9]. Recently, clinical applications of ALA-PDD have expanded to a wide variety of cancer types [10–13]. ALA-PDT has been successfully used to treat patients with various neoplastic and non-neoplastic diseases [14,15]. However, it has been reported that the cytotoxic effect of ALA-PDT is attenuated in cells with low expression of PEPT1, a transporter that allows ALA into cells, cells with overexpression of ABCG2, a transporter that exports PpIX, and cells expressing mutant p53 [4,16,17]. Therefore, it is essential to develop a novel strategy to enhance the cytotoxic effect of ALA-PDT.

We recently found that the Schiff base derivative *N*-3',5'-dichloro-2'-hydroxybenzylidene-2-chloro-4-nitroaniline, TX-816, could significantly increase the effect of ALA-PDT by accelerating intracellular PpIX accumulation [18]. However, TX-816 was unstable in the aqueous solution and was quickly hydrolyzed into 3,5-dichlorosalicylaldehyde (DCSA) and 2-chloro-4-nitroaniline (CAN). Therefore, we searched for a method to enhance the hydrolysis resistance of TX-816 derivatives. In this study, we reported the enhanced cytocidal activity of ALA-PDT against human cancer cells using novel derivatives of TX-816.

Experimentals

Materials

All solvents and chemicals were purchased from Wako Pure Chemical Industries (Osaka, Japan), Tokyo Chemical Industries (Tokyo, Japan), and Sigma-Aldrich (St. Louis, MO, USA). ALA was purchased from Tokyo Chemical Industries. During chemical synthesis, the progress of the reactions was monitored using Merck silica gel 60 F_{254} TLC plates (Merck, Darmstadt, Germany) with ethyl acetate (EtOAc)/n-hexane. Column chromatography was performed using silica-gel 60N purchased from Kanto Chemical (Tokyo, Japan). ^{1}H-NMR spectra were recorded using JNM-EX-400 (JEOL, Tokyo, Japan) in a deuterated solvent. Data were reported as follows: chemical shift, multiplicity (s = singlet, d = doublet, t = triplet, q = quartet, dd = double doublet, m = multiplet, brs = broad singlet), coupling constants (Hz), and integration. Broad singlet peaks, speculated to arise from OH protons, were also noted. The purity of all final compounds was confirmed at >95% using high performance liquid chromatography (JASCO PU-2089 Plus: Tokyo, Japan) with detection at 330 nm. Gradient elution was performed using mixtures of solvent n-hexane and chloroform ($CHCl_3$) on a TSKgel Amide-80 3 μm column (4.6 mm I.D.×15 cm) at a flow rate of 0.5 mL/min. The column temperature was not controlled. High-resolution mass

spectroscopy (HRMS) was performed using Waters LCT Premier XE (Waters, Milford, MA, USA) and Waters ACQUITY UPLC (Waters, Milford, MA, USA).

Synthesis of Schiff base derivatives

TX-816

DCSA (504 mg, 2.64 mmol) was dissolved in dry toluene (30 mL). CNA (683 mg, 3.96 mmol, 1.5 eq.) was added to the solution on the ice bath. The reaction mixture was warmed up to room temperature and refluxed for 24 h using Dean-Stark apparatus. After the reaction, the solvent was evaporated. The residue was purified by flash silica-gel column chromatography using EtOAc/n-hexane. TX-816 was afforded as a red solid (266 mg, 0.77 mmol, 29%). ^{1}H-NMR (400 MHz, DMSO-d6): δ 13.5 (brs, 1H), 9.14 (s, 1H), 8.48 (d, J = 2.4 Hz, 1H), 8.38 (dd, J = 8.8, 2.4 Hz, 1H), 7.87 (d, J = 2.4 Hz, 1H), 7.84 (s, 1H), 7.82 (d, J = 2.8 Hz, 1H); HRMS (ESI+) *m/z* calcd. for $C_{13}H_8N_2O_3Cl_3$ $[M + H]^+$ 344.9601, found 344.9617.

Compound **1** (UTX-122)

Aniline (220 μL, 2.40 mmol, 1.5 eq.) and dried 3A molecular sieves (975 mg) were mixed with DCSA (305 mg, 1.60 mmol) dissolved in dry toluene (15 mL) on the ice bath. The reaction mixture was warmed up to room temperature and refluxed for 3 h. After evaporation, the residue was purified by flash silica-gel column chromatography using EtOAc/n-Hexane. Compound **1** (UTX-122) was afforded as an orange solid (415 mg, 1.56 mmol, 98%). ^{1}H-NMR (400 MHz, DMSO-D6): δ 9.01 (d, J = 3.6 Hz, 1H), 7.69–7.73 (m, 2H), 7.46-7.48 (m, 4H), 7.33–7.36 (m, 1H); HRMS (ESI-TOF) *m/z* calcd. for $C_{13}H_{10}NOCl_2$ $[M + H]^+$ 266.0139, found 266.0152.

Compound **2** (UTX-123)

Compound **2** (UTX-123) was synthesized from *p*-toluidine (186 mg, 1.74 mmol) in 94% yield using the method described for the preparation of UTX-122. ^{1}H-NMR (400 MHz, DMSO-d6): δ 14.7 (brs, 1H), 9.02 (s, 1H), 7.72 (d, J = 2.4 Hz, 1H), 7.70 (d, J = 2.8 Hz, 1H), 7.40 (d, J = 8.8 Hz, 2H), 7.30 (d, J = 8.0 Hz, 2H), 2.34 (s, 3H); HRMS (ESI-TOF) *m/z* calcd. for $C_{14}H_{12}NOCl_2$ $[M + H]^+$ 280.0296, found 280.0298.

Compound **3** (UTX-124)

Compound **3** (UTX-124) was synthesized from 4-ethylaniline (400 μL, 3.20 mmol) in 95% yield using the method described for the preparation of UTX-122. ^{1}H-NMR (400 MHz, DMSO-d6): δ 9.01 (s, 1H), 7.71 (d, J = 2.8 Hz, 1H), 7.69 (d, J = 2.0 Hz, 1H), 7.40 (d, J = 8.8 Hz, 2H), 7.32 (d, J = 8.4 Hz, 2H), 2.63 (dd, J = 7.6 Hz, 2H), 1.18 (t, J = 7.6 Hz, 3H); HRMS (ESI-TOF) *m/z* calcd. for $C_{15}H_{14}NOCl_2$ $[M + H]^+$ 294.0452, found 294.0439.

Compound **4** (UTX-125)

Compound **4** (UTX-125) was synthesized from 4-propylaniline (231 μL, 1.57 mmol) in 100% yield using the method described for the preparation of UTX-122. ^{1}H-NMR (400 MHz, DMSO-d6): δ 9.01 (s, 1H), 7.71 (d, J = 1.6 Hz, 1H), 7.69 (d, J = 1.6 Hz, 1H), 7.40 (d, J = 8.4 Hz, 2H), 7.30 (d, J = 8.0 Hz, 2H), 2.58 (t, J = 7.6 Hz, 2H), 1.54–1.63 (m, 2H), 0.88 (t, J = 7.4 Hz, 3H); HRMS (ESI-TOF) *m/z* calcd. for $C_{16}H_{16}NOCl_2$ $[M + H]^+$ 308.0609, found 308.0613.

Compound **5** (UTX-126)

Compound **5** (UTX-126) was synthesized from 4-butylaniline (415 μL, 2.62 mmol) in 95% yield using the method described for the preparation of UTX-122. ^{1}H-NMR (400 MHz, DMSO-d6): δ 14.7 (brs, 1H), 9.02 (s, 1H), 7.72 (d, J = 2.8 Hz, 1H), 7.70 (d, J = 2.4 Hz, 1H), 7.41 (d, J = 8.0 Hz, 2H), 7.31 (d, J = 8.0 Hz, 2H), 2.63 (t, J = 9.2 Hz, 2H), 1.53–1.60 (m, 2H), 1.26–1.35 (m, 2H), 0.90 (t, J = 7.6 Hz, 3H); HRMS (ESI-TOF) *m/z* calcd. for $C_{17}H_{18}NOCl_2$ $[M + H]^+$ 322.0765, found 322.0750.

Compound **6** (UTX-127)

Compound **6** (UTX-127) was synthesized from 4-pentylaniline (185 μL, 1.05 mmol) in 97% yield using the method described for the preparation of UTX-122. ^{1}H-NMR (400 MHz, DMSO-d6): δ 9.01 (s, 1H), 7.70 (d, J = 8.0 Hz, 2H), 7.40 (d, J = 6.8 Hz, 2H), 7.30 (d, J = 7.6 Hz, 2H), 2.59 (t, J = 7.6 Hz, 2H), 1.53–1.60 (m, 2H), 1.27–1.30 (m, 4H), 0.84 (t, J = 6.2 Hz, 3H); HRMS (ESI-TOF) *m/z* calcd. for $C_{18}H_{20}NOCl_2$ $[M + H]^+$ 336.0922, found 336.0938.

Compound **7** (UTX-128)

Compound **7** (UTX-128) was synthesized from *p*-hexylaniline (400 μL, 2.09 mmol) in 47% yield using the method described for the preparation of UTX-122. ^{1}H-NMR (400 MHz, DMSO-d6): δ 14.7 (brs, 1H), 9.01 (s, 1H), 7.71 (d, J =2.8 Hz, 1H), 7.69 (d, J = 2.8 Hz, 1H), 7.39 (d, J = 8.4 Hz, 2H), 7.29 (d, J = 8.4 Hz, 2H), 2.59 (t, J = 7.8 Hz, 2H), 1.52–1.57 (m, 2H), 1.23–1.29 (m, 6H), 0.83 (t, J = 7.0 Hz, 3H); HRMS (ESI-TOF) *m/z* calcd. for $C_{19}H_{22}NOCl_2$ $[M + H]^+$ 350.1078, found 350.1067.

Compound **8** (UTX-129)

2-Hydroxy-4-methoxybenzaldehyde (MeOSA) (300 mg, 1.97 mmol) was dissolved in dry 1,2-dichloroethane (10 mL). Aniline (275 μL, 3.00 mmol, 1.5 eq.) and dried 3A molecular sieves (905 mg) were added to the mixture on the ice bath. The reaction mixture was treated as described above. Compound **8** (UTX-129) was afforded as a yellow solid (259 mg, 1.14 mmol, 58%). ^{1}H-NMR (400 MHz, DMSO-D6): δ 13.6 (brs, 1H), 8.84 (s, 1H), 7.50 (d, J =8.8 Hz, 1H), 7.41 (t, J = 8.2 Hz, 2H), 7.34 (d, J = 7.2 Hz, 2H), 7.24 (t, J = 7.2 Hz, 1H), 6.52 (d, J = 8.4 Hz, 1H), 6.46 (d, J = 2.0 Hz, 1H), 3.77 (s, 3H); HRMS (ESI-TOF) *m/z* calcd. for $C_{14}H_{14}NO_2$ $[M + H]^+$ 228.1025, found 228.1028.

Compound **9** (UTX-130)

Compound **9** (UTX-130) was synthesized from *p*-toluidine (194 mg, 1.81 mmol) in 61% yield using the method described for the preparation of UTX-129. ^{1}H-NMR (400 MHz, DMSO-D6): δ 8.82 (s, 1H), 7.48 (d, J =8.8 Hz, 1H), 7.25 (d, J = 8.4 Hz, 2H), 7.21 (d, J = 8.4 Hz, 2H), 6.51 (d, J = 8.8 Hz, 1H), 6.44 (d, J = 2.8 Hz, 1H), 3.77 (s, 3H), 2.29 (s, 3H); HRMS (ESI-TOF) *m/z* calcd. for $C_{15}H_{16}NO_2$ $[M + H]^+$ 242.1181, found 242.1177.

Compound **10** (UTX-131)

Compound **10** (UTX-131) was synthesized from 4-ethylaniline (150 μL, 1.20 mmol) in 82% yield using the method described for the preparation of UTX-129. ^{1}H-NMR (400 MHz, DMSO-D6): δ 13.8 (brs, 1H), 8.83 (s, 1H), 7.48 (d, J =8.8 Hz, 1H), 7.25 (q, J = 15.8, 7.9 Hz, 4H), 6.51 (d, J = 8.8 Hz, 1H), 6.44 (d, J = 2.4 Hz, 1H), 3.76 (s, 3H), 2.59 (q, J = 15.8, 7.9 Hz, 2H), 1.15 (t, J = 7.4 Hz, 3H); HRMS (ESI-TOF) *m/z* calcd. for $C_{16}H_{18}NO_2$ $[M + H]^+$ 256.1338, found 256.1326.

Compound **11** (UTX-132)

Compound **11** (UTX-132) was synthesized from 4-propylaniline (200 μL, 1.36 mmol) in 84% yield using the method described for the preparation of UTX-129. ^{1}H-NMR (400 MHz, DMSO-D6): δ 13.8 (brs, 1H), 8.83 (s, 1H), 7.48 (d, J =8.4 Hz, 1H), 7.26 (d, J = 8.8 Hz, 2H), 7.21 (d, J = 8.8 Hz, 2H), 6.51 (d, J = 8.8 Hz, 1H), 6.44 (d, J = 2.0 Hz, 1H), 3.76 (s, 3H), 2.53 (t, J = 7.4 Hz, 2H), 1.62–1.51 (m, 2H), 0.86 (t, J = 7.6 Hz, 3H); HRMS (ESI-TOF) *m/z* calcd. for $C_{17}H_{20}NO_2$ $[M + H]^+$ 270.1494, found 270.1481.

Compound **12** (UTX-133)

Compound **12** (UTX-133) was synthesized from 4-butylaniline (420 μL, 2.63 mmol) in 44% yield using the method described for the preparation of UTX-129. ^{1}H-NMR (400 MHz, DMSO-D6): δ 8.82 (s, 1H), 7.48 (d, J =8.8 Hz, 1H), 7.26 (d, J = 6.4 Hz, 2H), 7.21 (d, J = 8.8 Hz, 2H), 6.51 (d, J = 8.4 Hz, 1H), 6.44 (d, J = 2.8 Hz, 1H), 3.76 (s, 3H), 2.55 (t, J = 7.8 Hz, 2H), 1.55–1.48 (m, 2H), 1.31–1.19 (m, 2H), 0.86 (t, J = 7.4 Hz, 3H); HRMS (ESI-TOF) *m/z* calcd. for $C_{18}H_{22}NO_2$ $[M + H]^+$ 284.1651, found 284.1662.

Compound **13** (UTX-134)

Compound **13** (UTX-134) was synthesized from 4-pentylaniline (310 μL, 1.75 mmol) in 63% yield using the method described for the preparation of UTX-129. ^{1}H-NMR (400 MHz, DMSO-D6): δ 8.82 (s, 1H), 7.48 (d, J =8.8 Hz, 1H), 7.26 (d, J = 8.0 Hz, 2H), 7.21 (d, J = 8.4 Hz, 2H), 6.51 (d, J = 8.4 Hz, 1H), 6.44 (d, J = 2.4 Hz, 1H), 3.76 (s, 3H), 2.55 (t, J = 7.8 Hz, 2H), 1.58–1.50 (m, 2H), 1.32–1.21 (m, 4H), 0.82 (t, J = 7.0 Hz, 3H); HRMS (ESI-TOF) *m/z* calcd. for $C_{19}H_{24}NO_2$ $[M + H]^+$ 298.1807, found 298.1795.

Compound **14** (UTX-135)

Compound **14** (UTX-135) was synthesized from *p*-hexylaniline (335 µL, 1.74 mmol) in 68% yield using the method described for the preparation of UTX-129. ^{1}H-NMR (400 MHz, DMSO-D6): δ 8.82 (s, 1H), 7.48 (d, J =8.8 Hz, 1H), 7.26 (d, J = 8.8 Hz, 2H), 7.21 (d, J = 8.8 Hz, 2H), 6.51 (d, J = 8.4 Hz, 1H), 6.44 (d, J = 2.8 Hz, 1H), 3.77 (s, 3H), 2.55 (t, J = 7.4 Hz, 2H), 1.55–1.49 (m, 2H), 1.27–1.21 (m, 6H), 0.82 (t, J = 6.8 Hz, 3H); HRMS (ESI-TOF) *m/z* calcd. for $C_{20}H_{26}NO_2$ $[M + H]^+$ 312.1964, found 312.1950.

Cells and cell culture

The poorly differentiated gastric cancer cell line MKN-45 was provided by Dr. Suzuki (Fukushima Medical College, Fukushima, Japan). As per our previous report, the MKN-45 cell lines resistant to ALA-PDT were established by repeated treatment with 5 min PDT, after exposure with 200 µM ALA and sub-cloning [18]. Briefly, MKN-45 cells were seeded into a 35-mm dish and incubated with 200 µM ALA for 4 h. The cells were exposed to red LED light (630 nm, 80 mW/cm^2) for 5 min. The surviving and re-growing cells, which were resistant to ALA, were collected and seeded into a new dish, treated again with ALA-PDT (R and R400), and re-seeded into a new 15-cm dish after each treatment. Colonies of re-growing resistant cells were picked up and cultured (R13). R400 is a cell line resistant to 5 min PDT using 400 µM ALA. Both R and R400 were repeatedly treated with ALA-PDT over 3 months.

Cells were maintained in RPMI-1640 medium supplemented with 10% (v/v) heat-inactivated fetal bovine serum and 50 µg/mL kanamycin at 37 °C in a humidified atmosphere containing 5% CO_2.

ALA-PDT sensitivity assay by LED irradiation

Cells were seeded at a density of 5×10^3 cells/well in a 96-well plate and cultured at 37 °C in 5% CO_2 for 24 h. Test compounds such as DCSA, MeOSA, DCSA-based 4-alkyl aniline derivatives, and MeOSA-based 4-alkyl aniline were dissolved in DMSO and added to the culture medium at 10 µM. The final concentration of DMSO in the culture medium was 0.5%. Thereafter, serial dilutions of ALA were added to the culture medium at concentrations between 7.8 and 1,000 µM. After 4 h of incubation, the medium was replaced by a completely fresh medium. Then, the 96-well plate was exposed to LED irradiation (630 nm, 80 mW/cm^2) emitted by an LED irradiation unit provided by SBI ALA PROMO (Tokyo, Japan) for 5 min. The LED light spot was an equally illuminated rectangular spot measuring 128 × 86 mm covering the whole area of the 96-well culture plate. For each concentration, triplicate wells were used and all assays were performed at least three times.

After LED irradiation, the cells were further incubated for 48–72 h, and the cell viability was measured by a colorimetric assay using Cell Counting Kit-8 (Dojindo Laboratories, Kumamoto, Japan) according to the manufacturer's instructions. After 72 h of incubation, the medium was replaced by a fresh medium containing the WST-8 reagent. After 3 h, the absorbance in each well was

measured at 450 nm, using a microplate spectrophotometer, ImmunoMini NJ-2300 (BioTec, Tokyo, Japan, Tokyo, Japan).

The percentage of cell growth inhibition was calculated by applying the following formula: cell growth inhibition (%) = (1-[T/C]) × 100, where C and T are the mean absorbance values of the control and treated groups, respectively. The IC_{50} value was determined graphically from the dose-response curve with at least three drug concentration points.

Measurement of intracellular PpIX

The cells (2×10^6 cells) were seeded in 6-cm dishes and incubated for 24 h. DCSA, MeOSA, DCSA-based 4-alkyl aniline derivatives, and MeOSA-based 4-alkyl aniline derivatives were added to the medium at the stated concentrations before ALA addition. All treatments were performed in triplicate. After 4 h of incubation, the cells were harvested using 2 mL of 0.25% trypsin-1 mM EDTA. A cell suspension was collected in a 5-mL tube and centrifuged at 800 rpm for 5 min. The supernatant was aspirated and the cells were washed with phosphate-buffered saline. Finally, the cell pellet was suspended in 500 µL of 2.5% Triton X-100 solution and the cell suspension was transferred into a 0.5-mL micro tube, incubated for 5 min at room temperature, homogenized using Physcotron NS36D micro homogenizer (Microtec, Chiba, Japan), and centrifuged at 15,000 rpm for 10 min. The fluorescence intensity of PpIX in the supernatant was measured using a SEC2000-UV/VIS spectrophotometer (BAS, Tokyo, Japan: excitation, 410 nm; emission, 634 nm).

Evaluation of chemical stability by gas chromatography-mass spectrometry

The stability of 4-alkyl aniline derivatives and TX-816 was evaluated by gas chromatography-mass spectrometry (GC/MS) using the Agilent 7820A GC system coupled to the Agilent 5977E MSD system (Agilent Technologies, CA, USA). 1,5-Diphenyl-1,4-pentadien-3-one as an internal control was dissolved in 10% water/90% DMSO at 1.2 mM. The samples tested were dissolved at concentrations from 5 to 10 mM with the solvent including an internal control. Subsequently, the samples were immediately sonicated for 5 min. Then, the sample solutions were filtrated with a syringe filter (Minisart Syringe Filter, 0.2 µm, Sartorius AG, Göttingen, Germany) and settled at room temperature until measurement by GC/MS analysis. After appropriate incubation time, an aliquot of the sample solution was separated by GC system and all peaks corresponding to each compound including an internal control were identified by ion-fragment pattern based on a single quadrupole mass spectrometer with an electrospray ionization source. Separation was achieved with Ultra Inert Columns HP-5ms capillary GC column (30 m × 0.25 mm, 0.25 µm) (Agilent Technologies). Chromatographic conditions were as follows: the initial temperature was 50 °C or 120 °C for 0 min; it increased at a rate of 15 °C/min to 250 °C (15 min). The gas flow rate was 1.0 mL/min with helium used as a carrier gas. The amount of original compound and degraded materials were corrected with an internal control.

Results

Enhancing effect of DCSA-based or MeOSA-based 4-alkyl aniline derivatives on ALA-PDT

The synthesized Schiff base derivatives tested in this study are summarized in Fig. 1.

We investigated the enhancement effect of newly synthesized DCSA-based and MeOSA-based derivatives on ALA-PDT. When the IC_{50} values of ALA in the ALA-PDT sensitive assay were evaluated, the combination treatment of DCSA and DCSA-based all 4-alkyl aniline (C=0 to C=6) derivatives with ALA significantly enhanced the effect of ALA-PDT as compared with ALA alone (Fig. 2). On the other hand, the enhancing effect of MeOSA was less than that of DCSA and its derivatives. Among the Schiff base derivatives, MeOSA-based 4-pentyl and 4-hexyl aniline derivatives (UTX-134 and UTX-135) showed a stronger ALA-PDT enhancing effect than the other derivatives, including DCSA-based all 4-alkyl aniline derivatives. Specifically, UTX-135 was significantly the most effective ALA-PDT sensitizer.

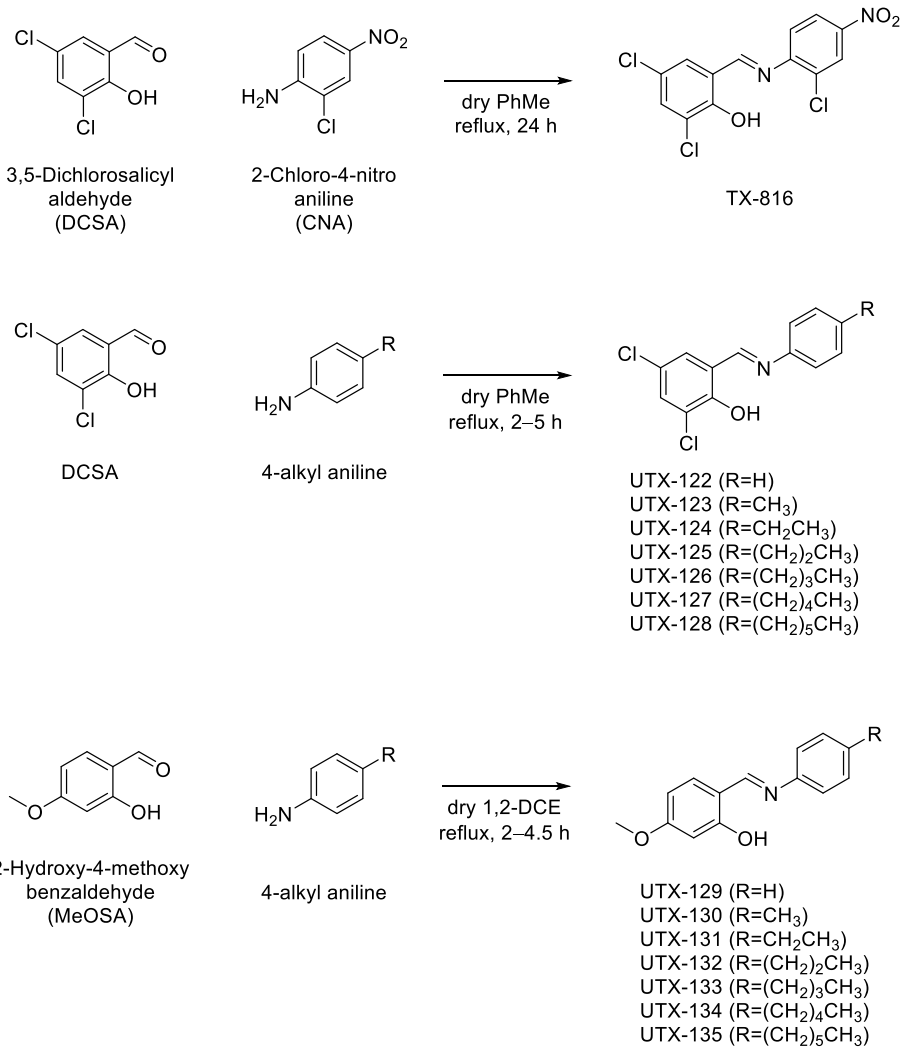

Fig. 1 Synthesis of TX-816, DCSA-based derivatives and MeOSA-based derivatives

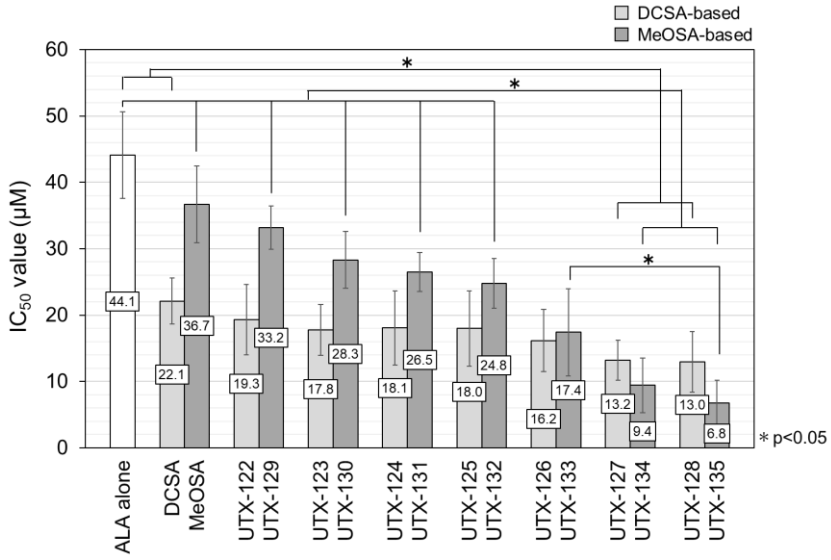

Fig. 2 Comparison of IC_{50} values in ALA-PDT sensitivity assay

Cells were seeded at a density of 5×10^3 cells/well in a 96-well plate. After 24 h of incubation, the compounds were added to the culture medium. Thereafter, serial dilutions of ALA (7.8–1,000 μM) were added to the culture medium. After 4 h of incubation, the 96-well plate was exposed to LED irradiation for 5 min and further incubated. Mean and standard deviation (error bars) of IC_{50} values were calculated by the data from three independent experiments, each made in triplicate.

Stability of DCSA-based and MeOSA-based 4-alkyl aniline derivatives in aqueous solution

TX-816 is very unstable in an aqueous solution and quickly produced aldehyde and amine by hydrolysis (Fig. 3) [18]. Therefore, we examined the stability of the 4-alkyl aniline derivatives using GC/MS system.

In 10%-water/90%-DMSO solvent (Fig. 4), TX-816 was rapidly hydrolyzed and > 50% of TX-816 was degraded within the first 5 min. After 100 min incubation, only 1.4% of the original TX-816 structure remained and almost the whole compound was converted into DCSA and CNA (55.0% and 43.6% respectively). In contrast, DCSA-based and MeOSA-based 4-butyl, 4-pentyl or 4-hexyl aniline derivatives (UTX-126–128 and UTX-133–135) were more stable than TX-816. Also, the MeOSA-based derivatives showed higher stability than the DCSA-based derivatives. After >1000 min of incubation, MeOSA-based derivatives were maintained original structures (> 80%).

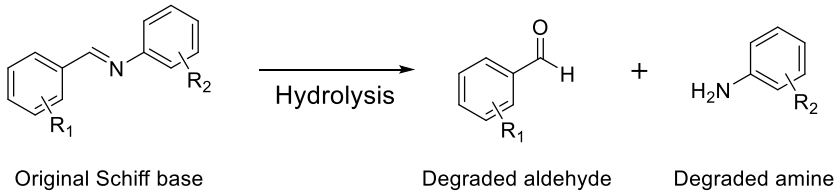

Fig. 3 Chemical structures of Schiff base and its degradation products

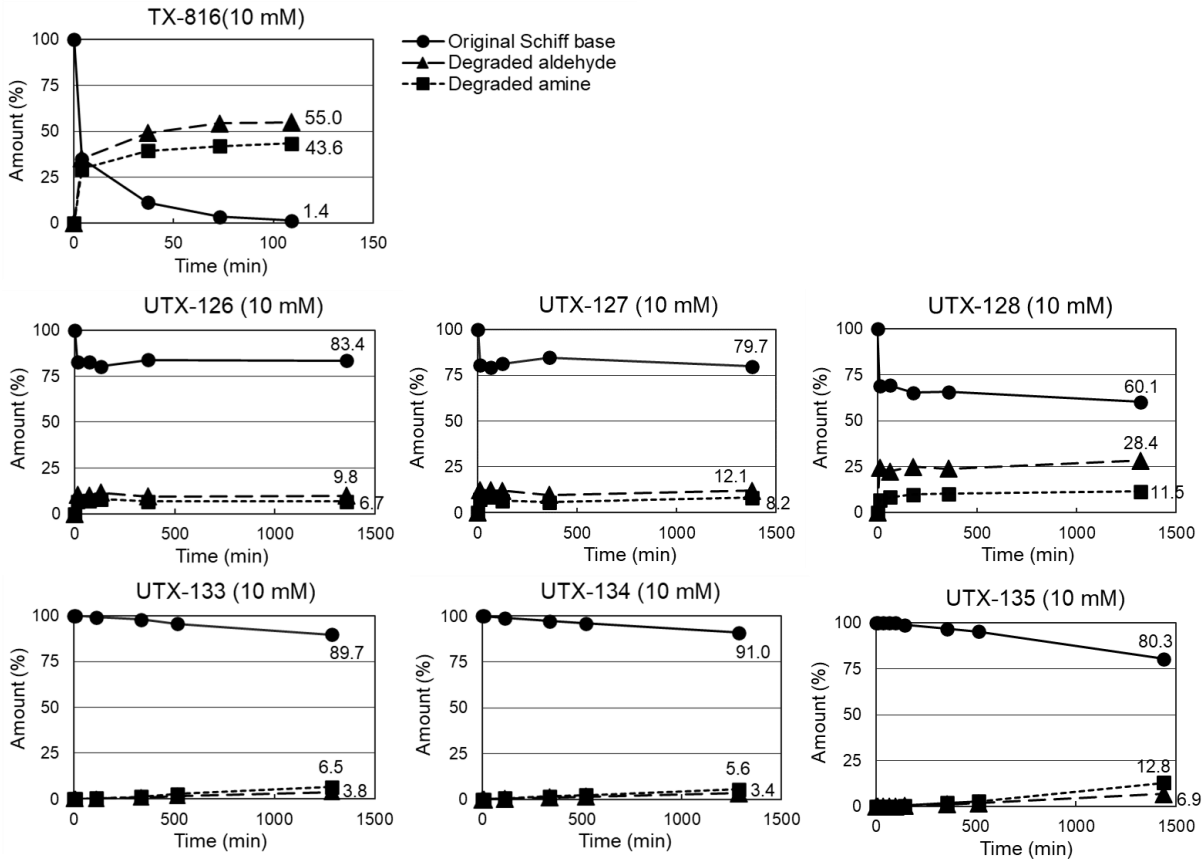

Fig. 4 Stability of Schiff base derivatives in 10% water/90% DMSO solvent

DCSA-based derivatives and MeOSA-based derivatives increased an intracellular PpIX accumulation in MKN-45 cells

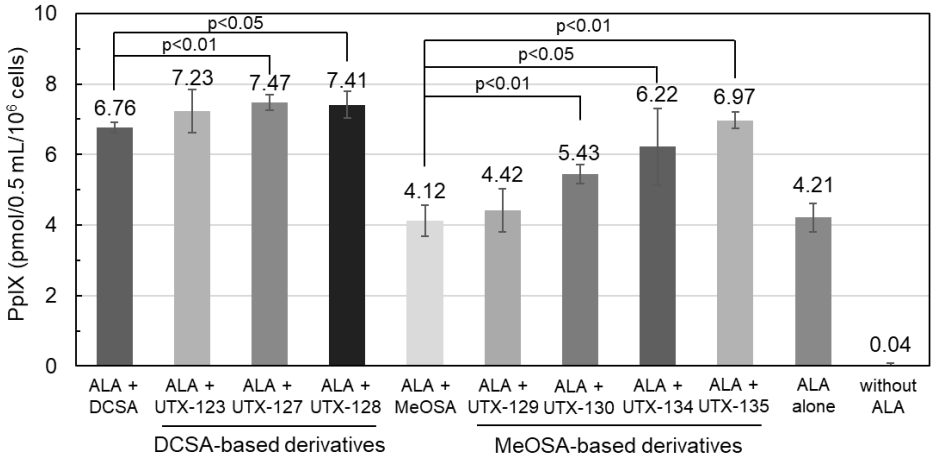

Fig. 5 Increased intracellular accumulation of PpIX in MKN-45 after combination treatment with ALA and Schiff base derivatives

MKN-45 cells were seeded at a density of 2 × 10^6 cells/well in a 6-cm dish. After 24 h of incubation, the compounds were added to the medium before ALA addition. After 4 h of incubation, the fluorescence intensity of PpIX was measured.

We investigated the relationship between the intracellular PpIX accumulation and the enhancement effect of DCSA-based and MeOSA-based derivatives on ALA-PDT. When MKN-45 cells were treated with 10 μM each compound and 50 μM ALA, the intracellular PpIX accumulation clearly increased in the cells treated with the 4-pentyl and 4-hexyl aniline derivatives (UTX-127, 128, 134, and 135) as compared to those treated with the corresponding original compounds as shown in Fig. 5. Interestingly, the enhancing activity of UTX-134 and UTX-135 on the intracellular PpIX accumulation tended to be slightly lower than that of the DCSA-based derivatives.

UTX-134 and UTX-135 enhanced treatment effects of ALA-PDT-resistant cells

Since TX-816 showed the effect of attenuating ALA-PDT resistance [18], we also examined the effect of DCSA-based and MeOSA-based derivatives on ALA-PDT-resistant cells. UTX-127, 128, 134, and 135 could effectively recover the sensitivity to ALA-PDT in R, R13, and R400 cells, which are MKN-45 cells that have acquired resistance (Fig. 6, Table 1). Specifically, UTX-134 and UTX-135 were more effective ALA-PDT sensitizers than DCSA-based derivatives.

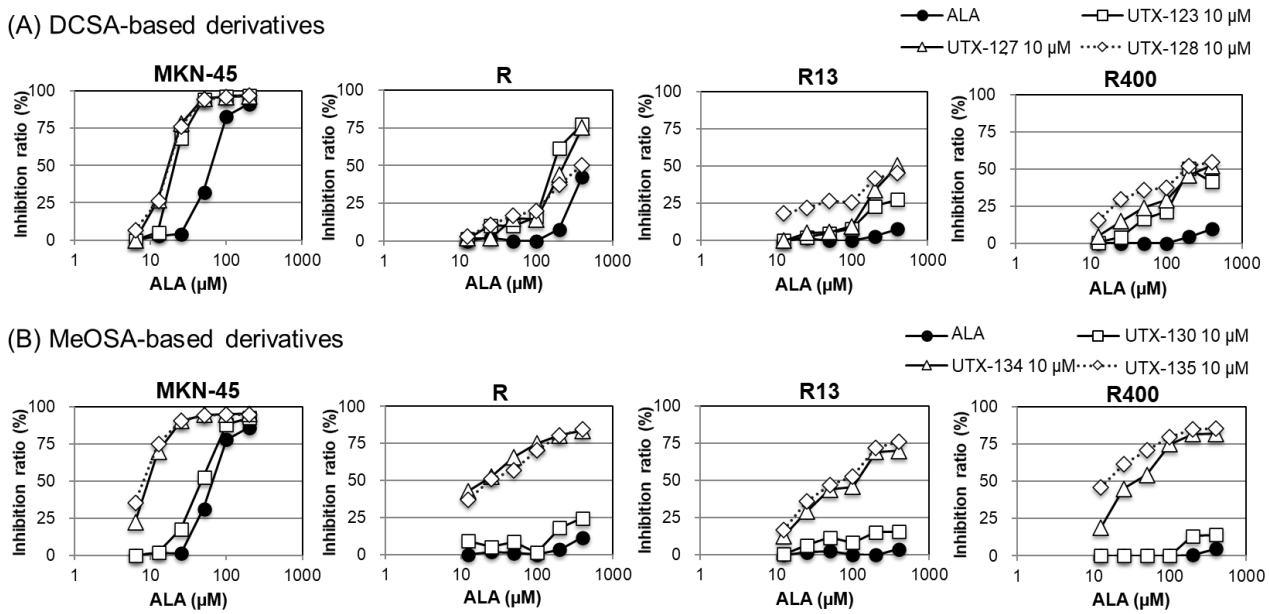

Fig. 6 The ALA-PDT enhancing effects of Schiff base derivatives in parental MKN-45 cells and its ALA-PDT-resistant cell lines

(A) DCSA-based derivatives. (B) MeOSA-based derivatives. Cells were seeded at a density of 5×10^3 cells/well in a 96-well plate. After 24 h of incubation, the compounds were added to the culture medium. Thereafter, serial dilutions of ALA were added to the culture medium as described in the "Experimentals" section. After 4 h of incubation, the 96-well plate was exposed to LED irradiation for 5 min and further incubated for 72 h.

Table 1 Comparison of IC_{50} values between DCSA-based and MeOSA-based derivatives in ALA-PDT sensitivity assay

	IC_{50} (μM) of ALA at 10 μM compound							
	DCSA-based derivative				MeOSA-based derivative			
Cells	ALA alone	UTX-123	UTX-127	UTX-128	ALA alone	UTX-130	UTX-134	UTX-135
MKN-45	59.8	22.8	17.7	17.3	63.5	47.3	10.0	8.20
R	>400	192.0	226.4	379.9	>400	>400	19.4	27.3
R13-2	>400	>400	378.3	>400	>400	>400	85.0	71.8
R400-1	>400	261.0	335.1	198.0	>400	>400	39.9	14.1

Discussion

In this study, we investigated the ALA-PDT enhancing activity of novel TX-816 derivatives and found that 4-alkyl aniline (C=0 to C=6) derivatives exhibited potent ALA-PDT enhancement effects (Fig. 2). In addition, the 4-butyl, 4-pentyl, and 4-hexyl aniline derivatives (UTX-126–128 and UTX-133–135) had higher stability than TX-816 (Fig. 4). This improved stability was probably due to the substitution of CNA with 4-alkyl aniline containing an electron-donating group [19, 20]. Interestingly, ALA-PDT enhancement effects of DCSA-based derivatives were relatively unaffected by the alkyl chain length, whereas those of MeOSA-based derivatives were significantly improved in a carbon-number dependent manner. Of these, the effects of UTX-134 and UTX-135 on ALA-PDT were better than that of the TX-816 and DCSA-based derivatives, and they also exhibited a potent activity on ALA-PDT-resistant cells (Fig. 6). Since DCSA-based derivatives were degraded more rapidly than MeOSA-based derivatives, the inhibition of PpIX emission by DCSA may have contributed to the ALA-PDT enhancement effect. This is also apparent from the finding that the intracellular PpIX levels were increased in the cells treated with DCSA-based derivatives, regardless of the length of the alkyl side chain (Fig. 5). On the contrary, because MeOSA-based derivatives are extremely stable, their ALA-PDT enhancement effects depend on PpIX emission inhibitory activities of compounds themselves. Therefore, it is speculated that the affinity to ABCG2 is increased as the alkyl side chain is extended, leading to an improvement in intracellular PpIX accumulation and PpIX emission inhibitory efficacy. However, the intracellular PpIX accumulation in MKN-45 cells treated with MeOSA-based derivatives tended to be lower than that in cells treated with DCSA-based derivatives (Fig. 5). The superior effects of UTX-134 and UTX-135 on ALA-PDT compared to DCSA-based derivatives were not reflected in the increased intracellular accumulation of PpIX. Although the ALA-PDT enhancement mechanism of these compounds has not yet been clarified, it cannot be ruled out that the intact Schiff base structure of MeOSA derivatives may directly promote the cytocidal activity of ALA-PDT [21]. Further studies are needed to determine the mechanism of ALA-PDT enhancement effects of the MeOSA-based derivatives.

Conclusion

UTX-134 and UTX-135 showed higher stability to an aqueous solution and a stronger ALA-PDT-enhancing effect than the TX-816 and DCSA-based derivatives. These results suggest that MeOSA-based derivatives are excellent lead compounds for the development of novel ALA-PDT enhancers.

Acknowledgement

We thank Tokushima Regional Base for Industry-Academia-Government joint Research for use of facilities. This study was partly supported by JSPS KAKENHI Grant Numbers JP26430160 (Yoshio Endo). This work was partly supported by the Extramural Collaborative Research Grant of Cancer Research Institute, Kanazawa University. Several research resources were kindly provided by the Joint Usage/Research Program of Cancer Research Institute, Kanazawa University.

References

1 X. Shi, C. Y. Zhang, J. Gao, Z. Wang, *Wiley Interdiscip. Rev. Nanomed. Nanobiotechnol.*, 2019, **11**(5), e1560.

2 R. S. Ajioka, J. D. Phillips, J. P. Kushner, *Biochim. Biophys. Acta.*, 2006, **1763**(7), 723–736.

3 M. Wachowska, A. Muchowicz, M. Firczuk, M. Gabrysiak, M. Winiarska, M. Wańczyk, K. Bojarczuk, J. Golab, *Molecules*, 2011, **16**(5), 4140–4164.

4 Y. Hagiya, H. Fukuhara, K. Matsumoto, Y. Endo, M. Nakajima, T. Tanaka, I. Okura, A. Kurabayashi, M. Furihata, K. Inoue, T. Shuin, S. Ogura, *Photodiagnosis Photodyn. Ther.*, 2013, **10**(3), 288–295.

5 K. Mahmoudi, K. L. Garvey, A. Bouras, G. Cramer, H. Stepp, J. G. Jesu Raj, D. Bozec, T. M. Busch, C. G. Hadjipanayis, *J. Neurooncol.*, 2019, **141**(3), 595–607.

6 Y. Tanaka, Y. Murayama, T. Matsumoto, H. Kubo, K. Harada, H. Matsuo, T. Kubota, K. Okamoto, E. Otsuji, *Oncol. Lett.*, 2020, **20**(4), 82.

7 Y. Sando, K. I. Matsuoka, Y. Sumii, T. Kondo, S. Ikegawa, H. Sugiura, M. Nakamura, M. Iwamoto, Y. Meguri, N. Asada, D. Ennishi, H. Nishimori, K. Fujii, N. Fujii, A. Utsunomiya, T. Oka, Y. Maeda, *Sci. Rep.*, 2020, **10**(1), 17237.

8 S. Kaneko, S. Kaneko, *Int. J. Biomed. Imaging*, 2016, 6135293.

9 S. Yamamoto, H. Fukuhara, T. Karashima, K. Inoue, *Photodiagnosis Photodyn Ther.*, 2020, **32**, 101999.

10 M. Motoori, M. Yano, K. Tanaka, K. Kishi, H. Takahashi, M. Inoue, T. Saito, K. Sugimura, Y. Fujiwara, O. Ishikawa, M. Sakon, *Oncology letters*, 2015, **10**(5), 3035–3039.

11 K. Kishi, Y. Fujiwara, M. Yano, M. Inoue, I. Miyashiro, M. Motoori, T. Shingai, K. Gotoh, H. Takahashi, S. Noura, T. Yamada, M. Ohue, H. Ohigashi, O. Ishikawa, *J. Surg. Oncol.*, 2012, **106**(3), 294–298.

12 H. Fukuhara, K. Inoue, A. Kurabayashi, M. Furihata, T. Shuin, *BMC Urol.*, 2015, 15:78.

13 K. Harada, Y. Murayama, H. Kubo, H. Matsuo, R. Morimura, H. Ikoma, H. Fujiwara, K. Okamoto, T. Tanaka, E. Otsuji, *Oncol. Lett.*, 2018, **16**(1), 821–828.
14 H. Hua, J. W. Cheng, W. B. Bu, J. Liu, W. W. Ma, N. Ni, J. Shi, B. R. Zhou, D. Luo, *Int. J. Biol. Sci.*, 2019, **15**(10), 2100–2109.
15 T. Yang, Y. Tan, W. Zhang, W. Yang, J. Luo, L. Chen, H. Liu, G. Yang, X. Lei, *Front. Cell Dev. Biol.*, 2020, **8**, 585132.
16 Y. Hagiya, Y. Endo, Y. Yonemura, K. Takahashi, M. Ishizuka, F. Abe, T. Tanaka, I. Okura, M. Nakajima, T. Ishikawa, S. Ogura, *Photodiagnosis Photodyn. Ther.*, 2012, **9**(3), 204–214.
17 Y. Hagiya, Y. Endo, Y. Yonemura, I. Okura, S. Ogura, *ALA-Porphyr. Sci.*, 2012, **1**, 23–31.
18 Y. Shinohara, Y. Endo, C. Abe, I. Shiba, M. Ishizuka, T. Tanaka, Y. Yonemura, S. Ogura, M. Tominaga, H. Yamada, Y. Uto, *Photodiagnosis Photodyn. Ther.*, 2017, **20**, 182–188.
19 J. Y. Mak, W. Xu, R. C. Reid, A. J. Corbett, B. S. Meehan, H. Wang, Z. Chen, J. Rossjohn, J. McCluskey, L. Liu, D. P. Fairlie, *Nat. Commun.*, 2017, **8**, 14599.
20 K. Bakalorz, Ł. Przypis, M. M. Tomczyk, M. Książek, R. Grzesik, N. Kuźnik, *Molecules*, 2020, **25**(5), 1257.
21 A. Kajal, S. Bala, S. Kamboj, N. Sharma, V. Saini, *J. Catal.*, 2013, **2013**.